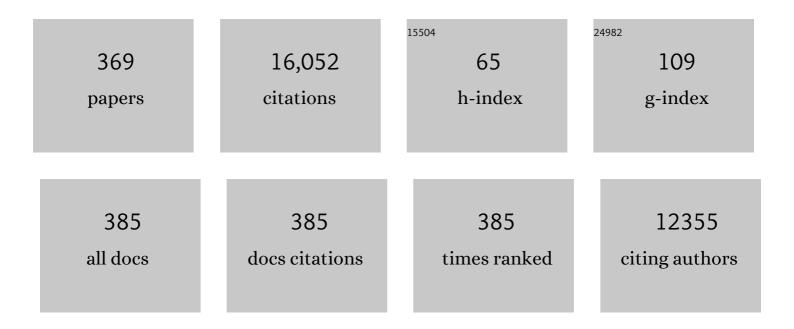
## M Parans Paranthaman

List of Publications by Year in descending order

Source: https://exaly.com/author-pdf/8621949/publications.pdf Version: 2024-02-01



#	Article	IF	CITATIONS
1	High critical current density superconducting tapes by epitaxial deposition of YBa2Cu3Ox thick films on biaxially textured metals. Applied Physics Letters, 1996, 69, 1795-1797.	3.3	944
2	Epitaxial YBa2Cu3O7 on Biaxially Textured Nickel (001): An Approach to Superconducting Tapes with High Critical Current Density. Science, 1996, 274, 755-757.	12.6	678
3	Irradiation-free, columnar defects comprised of self-assembled nanodots and nanorods resulting in strongly enhanced flux-pinning in YBa2Cu3O7â `Î films. Superconductor Science and Technology, 2005, 18, 1533-1538.	3.5	443
4	High-Performance High-Tc Superconducting Wires. Science, 2006, 311, 1911-1914.	12.6	395
5	Mesoporous TiO <sub>2</sub> –B Microspheres with Superior Rate Performance for Lithium Ion Batteries. Advanced Materials, 2011, 23, 3450-3454.	21.0	361
6	Band Gap Narrowing of Titanium Oxide Semiconductors by Noncompensated Anion-Cation Codoping for Enhanced Visible-Light Photoactivity. Physical Review Letters, 2009, 103, 226401.	7.8	347
7	Studies on Supercapacitor Electrode Material from Activated Lignin-Derived Mesoporous Carbon. Langmuir, 2014, 30, 900-910.	3.5	342
8	The RABiTS Approach: Using Rolling-Assisted Biaxially Textured Substrates for High-Performance YBCO Superconductors. MRS Bulletin, 2004, 29, 552-561.	3.5	247
9	Self-organized amorphous TiO2 nanotube arrays on porous Ti foam for rechargeable lithium and sodium ion batteries. Journal of Power Sources, 2013, 222, 461-466.	7.8	235
10	Role of Cation Ordering and Surface Segregation in High-Voltage Spinel LiMn <sub>1.5</sub> Ni <sub>0.5–<i>x</i></sub> M <sub><i>x</i></sub> O <sub>4</sub> (M = Cr, Fe, and Ga) Cathodes for Lithium-Ion Batteries. Chemistry of Materials, 2012, 24, 3720-3731.	6.7	202
11	Surface protonation and electrochemical activity of oxides in aqueous solution. Journal of the American Chemical Society, 1990, 112, 2076-2082.	13.7	197
12	Growth of biaxially textured buffer layers on rolled-Ni substrates by electron beam evaporation. Physica C: Superconductivity and Its Applications, 1997, 275, 266-272.	1.2	176
13	Low angle grain boundary transport in YBa2Cu3O7â^î^ coated conductors. Applied Physics Letters, 2000, 76, 1755-1757.	3.3	166
14	Conductors with controlled grain boundaries: An approach to the next generation, high temperature superconducting wire. Journal of Materials Research, 1997, 12, 2924-2940.	2.6	161
15	Solution-derived textured oxide thin films—a review. Superconductor Science and Technology, 2006, 19, R1-R21.	3.5	161
16	Big Area Additive Manufacturing of High Performance Bonded NdFeB Magnets. Scientific Reports, 2016, 6, 36212.	3.3	138
17	Electrical properties of epoxy resin based nano-composites. Nanotechnology, 2007, 18, 025703.	2.6	133
18	Recovery of Lithium from Geothermal Brine with Lithium–Aluminum Layered Double Hydroxide Chloride Sorbents. Environmental Science & Technology, 2017, 51, 13481-13486.	10.0	132

#	Article	IF	CITATIONS
19	High-Performance YBCO-Coated Superconductor Wires. MRS Bulletin, 2004, 29, 533-541.	3.5	131
20	Reverse micellar synthesis of cerium oxide nanoparticles. Nanotechnology, 2005, 16, 1960-1964.	2.6	131
21	Superconducting MgB2 films via precursor postprocessing approach. Applied Physics Letters, 2001, 78, 3669-3671.	3.3	130
22	Epitaxial superconductors on rolling-assisted biaxially-textured substrates (RABiTS): a route towards high critical current density wire. Applied Superconductivity, 1996, 4, 403-427.	0.5	129
23	MOD approach for the growth of epitaxial CeO2buffer layers on biaxially textured Ni–W substrates for YBCO coated conductors. Superconductor Science and Technology, 2003, 16, 1305-1309.	3.5	123
24	Binder Jetting: A Novel NdFeB Bonded Magnet Fabrication Process. Jom, 2016, 68, 1978-1982.	1.9	121
25	Deposition of biaxially-oriented metal and oxide buffer-layer films on textured Ni tapes: new substrates for high-current, high-temperature superconductors. Physica C: Superconductivity and Its Applications, 1997, 275, 155-161.	1.2	117
26	Superior Conductive Solid-like Electrolytes: Nanoconfining Liquids within the Hollow Structures. Nano Letters, 2015, 15, 3398-3402.	9.1	115
27	Far-Infrared Optical Conductivity Gap in SuperconductingMgB2Films. Physical Review Letters, 2001, 88, 027003.	7.8	112
28	Electrical Conductivity of the Manganese Chromite Spinel Solid Solution. Journal of the American Ceramic Society, 2005, 88, 1050-1053.	3.8	110
29	Aligned ZnO Nanorod Arrays Grown Directly on Zinc Foils and Zinc Spheres by a Low-Temperature Oxidization Method. ACS Nano, 2009, 3, 273-278.	14.6	108
30	Low-cost YBCO coated conductor technology. Superconductor Science and Technology, 2000, 13, 473-476.	3.5	107
31	Lithium Recovery from Aqueous Resources and Batteries: A Brief Review. Johnson Matthey Technology Review, 2018, 62, 161-176.	1.0	107
32	A Novel Electrolyte Salt Additive for Lithiumâ€lon Batteries with Voltages Greater than 4.7 V. Advanced Energy Materials, 2017, 7, 1601397.	19.5	103
33	Oxide ion electrolytes. Materials Science and Engineering B: Solid-State Materials for Advanced Technology, 1992, 12, 357-364.	3.5	102
34	Additive manufacturing of near-net-shape bonded magnets: Prospects and challenges. Scripta Materialia, 2017, 135, 100-104.	5.2	102
35	Cube-textured nickel substrates for high-temperature superconductors. Superconductor Science and Technology, 1998, 11, 945-949.	3.5	101
36	Recent progress in the fabrication of high-Jc tapes by epitaxial deposition of YBCO on RABiTS. Physica C: Superconductivity and Its Applications, 2001, 357-360, 903-913.	1.2	101

#	Article	IF	CITATIONS
37	Enhanced flux pinning by BaZrO3 and (Gd,Y)2O3 nanostructures in metal organic chemical vapor deposited GdYBCO high temperature superconductor tapes. Applied Physics Letters, 2009, 94, .	3.3	98
38	YBCO coated conductors by an MOD/RABiTS process. IEEE Transactions on Applied Superconductivity, 2003, 13, 2458-2461.	1.7	96
39	Orienting Oxygen Vacancies for Fast Catalytic Reaction. Advanced Materials, 2013, 25, 6459-6463.	21.0	96
40	Waste Tire Derived Carbon–Polymer Composite Paper as Pseudocapacitive Electrode with Long Cycle Life. ChemSusChem, 2015, 8, 3576-3581.	6.8	94
41	Effect of carbon-doping in bulk superconducting MgB2 samples. Physica C: Superconductivity and Its Applications, 2001, 355, 1-5.	1.2	92
42	Second Generation HTS Wire Based on RABiTS Substrates and MOD YBCO. IEEE Transactions on Applied Superconductivity, 2005, 15, 2611-2616.	1.7	92
43	In Situ Observation of Solid Electrolyte Interphase Formation in Ordered Mesoporous Hard Carbon by Small-Angle Neutron Scattering. Journal of Physical Chemistry C, 2012, 116, 7701-7711.	3.1	92
44	Uniform performance of continuously processed MOD-YBCO-coated conductors using a textured Ni–W substrate. Superconductor Science and Technology, 2003, 16, L19-L22.	3.5	89
45	Enhancement of dielectric strength in nanocomposites. Nanotechnology, 2007, 18, 325704.	2.6	89
46	Sustainable Potassium-Ion Battery Anodes Derived from Waste-Tire Rubber. Journal of the Electrochemical Society, 2017, 164, A1234-A1238.	2.9	88
47	Tire-derived carbon composite anodes for sodium-ion batteries. Journal of Power Sources, 2016, 316, 232-238.	7.8	85
48	Texture formation and grain boundary networks in rolling assisted biaxially textured substrates and in epitaxial YBCO films on such substrates. Micron, 1999, 30, 463-478.	2.2	84
49	Temperature Dependence of Aliovalent-Vanadium Doping in LiFePO <sub>4</sub> Cathodes. Chemistry of Materials, 2013, 25, 768-781.	6.7	83
50	LaCrO3-based coatings on ferritic stainless steel for solid oxide fuel cell interconnect applications. Surface and Coatings Technology, 2004, 177-178, 65-72.	4.8	82
51	Additive manufacturing of soft magnets for electrical machines—a review. Materials Today Physics, 2020, 15, 100255.	6.0	81
52	Enhancement of flux pinning and critical currents in YBa2Cu3O7â^î^ films by nanoscale iridium pretreatment of substrate surfaces. Journal of Applied Physics, 2005, 98, 114309.	2.5	80
53	Comparative Study of Thickness Dependence of Critical Current Density of Yba <sub>2</sub> Cu <sub>3</sub> O <sub>7–î</sub> on (100) SrTiO <sub>3</sub> and on Rolling-assisted Biaxially Textured Substrates. Journal of Materials Research, 2002, 17, 1750-1757.	2.6	79
54	High Jc YBCO films on biaxially textured Ni with oxide buffer layers deposited using electron beam evaporation and sputtering. Physica C: Superconductivity and Its Applications, 1998, 302, 87-92.	1.2	77

#	Article	IF	CITATIONS
55	Conductive surface modification of LiFePO4 with nitrogen-doped carbon layers for lithium-ion batteries. Journal of Materials Chemistry, 2012, 22, 4611.	6.7	76
56	Strengthened, biaxially textured Ni substrate with small alloying additions for coated conductor applications. Physica C: Superconductivity and Its Applications, 2002, 382, 251-262.	1.2	75
57	Epitaxial growth of La2Zr2O7 thin films on rolled Ni-substrates by sol–gel process for high Tc superconducting tapes. Physica C: Superconductivity and Its Applications, 2000, 336, 63-69.	1.2	74
58	Biaxially Textured YBa2Cu3O7-δ Conductors on Rolling Assisted Biaxially Textured Substrates with Critical Current Densities of 2-3 mA/cm2. Japanese Journal of Applied Physics, 1998, 37, L1379-L1382.	1.5	72
59	Growth of biaxially textured RE2O3buffer layers on rolled-Ni substrates using reactive evaporation for HTS-coated conductors. Superconductor Science and Technology, 1999, 12, 319-325.	3.5	72
60	Lithium malonatoborate additives enabled stable cycling of 5 V lithium metal and lithium ion batteries. Nano Energy, 2017, 40, 9-19.	16.0	72
61	Low cost Y-Ba-Cu-O coated conductors. IEEE Transactions on Applied Superconductivity, 2001, 11, 2927-2930.	1.7	70
62	Optimum lithium-ion conductivity in cubic Li7â^'xLa3Hf2â^'xTaxO12. Journal of Power Sources, 2012, 209, 184-188.	7.8	70
63	Tailored recovery of carbons from waste tires for enhanced performance as anodes in lithium-ion batteries. RSC Advances, 2014, 4, 38213.	3.6	70
64	Surface barriers, irreversibility line, and pancake vortices in an alignedHgBa2Ca2Cu3O8+l´superconductor. Physical Review B, 1995, 52, 4438-4445.	3.2	68
65	Additive manufacturing of anisotropic hybrid NdFeB-SmFeN nylon composite bonded magnets. Journal of Magnetism and Magnetic Materials, 2018, 467, 8-13.	2.3	68
66	YBa <sub>2</sub> Cu <sub>3</sub> O <sub>7-<i>y</i></sub> â^'coated conductors with high engineering current density. Journal of Materials Research, 2000, 15, 2647-2652.	2.6	65
67	A novel method combining additive manufacturing and alloy infiltration for NdFeB bonded magnet fabrication. Journal of Magnetism and Magnetic Materials, 2017, 438, 163-167.	2.3	65
68	Preparation of Cr-doped Y3Al5O12 phosphors by heterogeneous precipitation methods and their luminescent properties. Materials Research Bulletin, 2000, 35, 217-224.	5.2	64
69	Chemical and Electrochemical Lithiation of LiVOPO <sub>4</sub> Cathodes for Lithium-Ion Batteries. Chemistry of Materials, 2014, 26, 3849-3861.	6.7	63
70	Vortex fluctuations, magnetic penetration depth, andHc2in Hg- and Tl-based high-Tcsuperconductors. Physical Review B, 1993, 48, 14031-14034.	3.2	61
71	Analysis of flux pinning inYBa2Cu3O7â~δfilms by nanoparticle-modified substrate surfaces. Physical Review B, 2006, 74, .	3.2	60
72	Single-step synthesis of bulk HgBa2Ca2Cu3O8+Î′. Physica C: Superconductivity and Its Applications, 1994, 222, 7-12.	1.2	59

#	Article	IF	CITATIONS
73	Spontaneous Growth of ZnCO <sub>3</sub> Nanowires on ZnO Nanostructures in Normal Ambient Environment: Unstable ZnO Nanostructures. Chemistry of Materials, 2010, 22, 149-154.	6.7	58
74	High performance Cr, N-codoped mesoporous TiO <sub>2</sub> microspheres for lithium-ion batteries. Journal of Materials Chemistry A, 2014, 2, 1818-1824.	10.3	58
75	A POM–organic framework anode for Li-ion battery. Journal of Materials Chemistry A, 2015, 3, 22989-22995.	10.3	58
76	Insights into the Enhanced Cycle and Rate Performances of the Fâ€Substituted P2â€Type Oxide Cathodes for Sodiumâ€Ion Batteries. Advanced Energy Materials, 2020, 10, 2000135.	19.5	57
77	Monolithic graded-refractive-index glass-based antireflective coatings: broadband/omnidirectional light harvesting and self-cleaning characteristics. Journal of Materials Chemistry C, 2015, 3, 5440-5449.	5.5	55
78	Synthesis and magnetic characterization of the high-Tc superconducting compound HgBa2CuO4+δ. Physica C: Superconductivity and Its Applications, 1993, 213, 271-275.	1.2	54
79	Fabrication and characterization of brookite-rich, visible light-active TiO2 films for water splitting. Applied Catalysis B: Environmental, 2009, 93, 90-95.	20.2	54
80	Bend strain tolerance of critical currents for YBa2Cu3O7 films deposited on rolled-textured (001)Ni. Applied Physics Letters, 1998, 73, 1904-1906.	3.3	53
81	La0.7Sr0.3MnO3: A single, conductive-oxide buffer layer for the development of YBa2Cu3O7â <sup>~°</sup> δ coated conductors. Applied Physics Letters, 2001, 79, 2205-2207.	3.3	53
82	Nitrogenâ€Enriched Carbons from Alkali Salts with High Coulombic Efficiency for Energy Storage Applications. Advanced Energy Materials, 2013, 3, 708-712.	19.5	51
83	Flux-pinning characteristics as a function of density of columnar defects comprised of self-assembled nanodots and nanorods in epitaxial YBa2Cu3O7â^1´films for coated conductor applications. Physica C: Superconductivity and Its Applications, 2007, 457, 41-46.	1.2	50
84	Fabrication of long lengths of YBCO coated conductors using a continuous reel-to-reel dip-coating unit. IEEE Transactions on Applied Superconductivity, 2001, 11, 3146-3149.	1.7	49
85	Enhanced flux pinning in MOCVD-YBCO films through Zr additions: systematic feasibility studies. Superconductor Science and Technology, 2010, 23, 014005.	3.5	49
86	A surfactant and template-free route for synthesizing ceria nanocrystals with tunable morphologies. Journal of Materials Chemistry, 2010, 20, 7776.	6.7	49
87	High temporal stability of supercurrents in MgB2materials. Superconductor Science and Technology, 2001, 14, L17-L20.	3.5	48
88	Superconducting magnesium diboride films on Si with TcOâ^¼24 K grown via vacuum annealing from stoichiometric precursors. Applied Physics Letters, 2001, 79, 2603-2605.	3.3	48
89	A high performance hybrid battery based on aluminum anode and LiFePO <sub>4</sub> cathode. Chemical Communications, 2016, 52, 1713-1716.	4.1	48
90	Membraneâ€Based Gas Separation Accelerated by Hollow Nanosphere Architectures. Advanced Materials, 2017, 29, 1603797.	21.0	48

M Parans Paranthaman

#	Article	IF	CITATIONS
91	Fabrication of highly dense isotropic Nd-Fe-B nylon bonded magnets via extrusion-based additive manufacturing. Additive Manufacturing, 2018, 21, 495-500.	3.0	48
92	High Critical Current Density YBa2Cu3O x Tapes Using the RABiTs Approach. Journal of Superconductivity and Novel Magnetism, 1998, 11, 481-487.	0.5	47
93	Bis(trimethylsilyl) 2-fluoromalonate derivatives as electrolyte additives for high voltage lithium ion batteries. Journal of Power Sources, 2019, 412, 527-535.	7.8	47
94	Inter- and intragrain transport measurements in YBa2Cu3O7â^'x deformation textured coated conductors. Applied Physics Letters, 2001, 79, 3998-4000.	3.3	45
95	In situ TEM observation of the electrochemical lithiation of N-doped anatase TiO <sub>2</sub> nanotubes as anodes for lithium-ion batteries. Journal of Materials Chemistry A, 2017, 5, 20651-20657.	10.3	45
96	Properties of the chemically characterized thallium cuprate superconductors. Physica C: Superconductivity and Its Applications, 1990, 171, 135-146.	1.2	44
97	Lanthanum zirconate: A single buffer layer processed by solution deposition for coated conductor fabrication. Journal of Materials Research, 2002, 17, 2181-2184.	2.6	44
98	Chemical solution deposition of lanthanum zirconate barrier layers applied to low-cost coated-conductor fabrication. Journal of Materials Research, 2004, 19, 2117-2123.	2.6	44
99	Synthesis and Characterization of Lithium Bis(fluoromalonato)borate for Lithiumâ€lon Battery Applications. Advanced Energy Materials, 2014, 4, 1301368.	19.5	43
100	Neutron powder diffraction study of the superconducting quaternary intermetallic compound YNi2B2C. Physica C: Superconductivity and Its Applications, 1994, 227, 143-150.	1.2	42
101	Crystal Chemistry of HgBa2Canâ ``1CunO2n+2+δ(n= 1, 2, 3, 4) Superconductors. Journal of Solid State Chemistry, 1996, 122, 221-230.	2.9	42
102	Microstructure of electron-beam-evaporated epitaxial yttria-stabilized zirconia/CeO2 bilayers on biaxially textured Ni tape. Physica C: Superconductivity and Its Applications, 1998, 307, 87-98.	1.2	42
103	Epitaxial YBa2Cu3O7 films on rolled-textured metals for high-temperature superconducting applications. Materials Science and Engineering B: Solid-State Materials for Advanced Technology, 1998, 56, 86-94.	3.5	42
104	Fabrication of Long Lengths of Epitaxial Buffer Layers on Biaxially Textured Nickel Substrates Using a Continuous Reelâ€ŧoâ€Reel Dipâ€Coating Unit. Journal of the American Ceramic Society, 2001, 84, 273-78.	3.8	41
105	The "filler effect†A study of solid oxide fillers with β-Li3PS4 for lithium conducting electrolytes. Solid State Ionics, 2015, 283, 75-80.	2.7	41
106	Structure of the superconducting gap in MgB2from point-contact spectroscopy. Superconductor Science and Technology, 2002, 15, 526-532.	3.5	40
107	Chemical Solution Deposition of Lanthanum Zirconate Buffer Layers on Biaxially Textured Ni–1.7% Fe–3% W Alloy Substrates for Coated-conductor Fabrication. Journal of Materials Research, 2002, 17, 1543-1549.	2.6	40
108	Vortex pinning and slow creep in high-JcÂMgB2thin films: a magnetic and transport study. Superconductor Science and Technology, 2005, 18, 970-976.	3.5	40

#	Article	IF	CITATIONS
109	Heteroepitaxial film silicon solar cell grown on Ni-W foils. Energy and Environmental Science, 2012, 5, 6052.	30.8	40
110	Manufacturing Processes for Permanent Magnets: Part l—Sintering and Casting. Jom, 2022, 74, 1279-1295.	1.9	40
111	Sol-gel Synthesis of LaAlO <sub>3</sub> ; Epitaxial Growth of LaAlO <sub>3</sub> Thin Films on SrTiO <sub>3</sub> (100). Journal of Materials Research, 1997, 12, 1017-1021.	2.6	39
112	Tire-derived carbon for catalytic preparation of biofuels from feedstocks containing free fatty acids. Carbon Resources Conversion, 2018, 1, 165-173.	5.9	38
113	Phase stability for thein situgrowth of Nd1+xBa2â^'xCu3Oy films using pulsed-laser deposition. Applied Physics Letters, 1999, 74, 96-98.	3.3	37
114	Comparing Cr, and N only doping with (Cr, N)-codoping for enhancing visible light reactivity of TiO2. Applied Catalysis B: Environmental, 2011, 110, 148-153.	20.2	37
115	Strong surface-pinning effects in polycrystallineHgBa2CuO4+l´superconductors. Physical Review B, 1994, 50, 3330-3336.	3.2	36
116	Probing microstructure and electrolyte concentration dependent cell chemistry <i>via operando</i> small angle neutron scattering. Energy and Environmental Science, 2019, 12, 1866-1877.	30.8	36
117	Binder jet additive manufacturing method to fabricate near net shape crack-free highly dense Fe-6.5 wt.% Si soft magnets. Heliyon, 2019, 5, e02804.	3.2	36
118	Chemical methods to identify the origin of oxidation in the thallium cuprate superconductors. Journal of Solid State Chemistry, 1990, 87, 479-482.	2.9	35
119	Equilibrium superconducting properties of grain-alignedHgBa2Ca2Cu3O8+δ. Physical Review B, 1995, 51, 11767-11772.	3.2	35
120	Continuous growth of epitaxial CeO2 buffer layers on rolled Ni tapes by electron beam evaporation. Physica C: Superconductivity and Its Applications, 1999, 316, 27-33.	1.2	34
121	Lithium aluminumâ€layered double hydroxide chlorides ( <scp>LDH</scp> ): Formation enthalpies and energetics for lithium ion capture. Journal of the American Ceramic Society, 2019, 102, 2398-2404.	3.8	34
122	Alternating current losses in biaxially textured YBa2Cu3O7â^î^films deposited on Ni tapes. Applied Physics Letters, 1997, 71, 2029-2031.	3.3	33
123	Electrical and magnetic properties of conductive Cu-based coated conductors. Applied Physics Letters, 2003, 83, 3963-3965.	3.3	33
124	Fabrication of high-critical current density Yba2Cu3O7â^'δ films using a fluorine-free sol gel approach. Journal of Materials Research, 2003, 18, 677-681.	2.6	33
125	Zinc Oxide Microtowers by Vapor Phase Homoepitaxial Regrowth. Advanced Materials, 2009, 21, 890-896.	21.0	33
126	Heteroepitaxial film crystal silicon on Al2O3: new route to inexpensive crystal silicon photovoltaics. Energy and Environmental Science, 2011, 4, 3346.	30.8	33

#	Article	IF	CITATIONS
127	Growth of biaxially oriented conductive LaNiO3 buffer layers on textured Ni tapes for high-Tc-coated conductors. Physica C: Superconductivity and Its Applications, 1999, 314, 105-111.	1.2	32
128	Effect of Ca doping on the electrical conductivity of the high temperature proton conductor LaNbO4. International Journal of Hydrogen Energy, 2012, 37, 12751-12759.	7.1	32
129	Carbon polyaniline capacitive deionization electrodes with stable cycle life. Desalination, 2019, 464, 25-32.	8.2	32
130	Preparation of YBCO Films on CeO <sub>2</sub> â€Buffered (001) YSZ Substrates by a Nonâ€Fluorine MOD Method. Journal of the American Ceramic Society, 2004, 87, 1669-1676.	3.8	31
131	Control of Flux Pinning in MOD YBCO Coated Conductor. IEEE Transactions on Applied Superconductivity, 2007, 17, 3347-3350.	1.7	31
132	Microstructure and magnetic properties of electrodeposited cobalt films. Journal of Materials Science, 2008, 43, 1644-1649.	3.7	31
133	Triangular Graphene Grain Growth on Cubeâ€Textured Cu Substrates. Advanced Functional Materials, 2011, 21, 3868-3874.	14.9	31
134	Long length fabrication of YBCO on rolling assisted biaxially textured substrates (RABiTS) using pulsed laser deposition. IEEE Transactions on Applied Superconductivity, 1999, 9, 2276-2279.	1.7	30
135	Epitaxial growth of gadolinium oxide on roll-textured nickel using a solution growth technique. Journal of Materials Research, 2000, 15, 621-628.	2.6	30
136	Degradation of superconducting properties in MgB2films by exposure to water. Superconductor Science and Technology, 2001, 14, 425-428.	3.5	30
137	Transverse compressive stress effect in Y-Ba-Cu-O coatings on biaxially textured Ni and Ni-W substrates. IEEE Transactions on Applied Superconductivity, 2003, 13, 3530-3533.	1.7	30
138	Synthesis and characterization of anodized titanium-oxide nanotube arrays. Journal of Materials Science, 2009, 44, 2820-2827.	3.7	30
139	Chemical solution derived planarization layers for highly aligned IBAD-MgO templates. Superconductor Science and Technology, 2014, 27, 022002.	3.5	30
140	Additive manufacturing of highly dense anisotropic Nd–Fe–B bonded magnets. Scripta Materialia, 2020, 183, 91-95.	5.2	30
141	Insight into the Solid Electrolyte Interphase Formation in Bis(fluorosulfonyl)Imide Based Ionic Liquid Electrolytes. Advanced Functional Materials, 2021, 31, 2008708.	14.9	30
142	Thermoelectric power and resistivity measurements on oxygen-annealedHgBa2Ca2Cu3O8+l´superconductors. Physical Review B, 1995, 51, 1330-1333.	3.2	29
143	Microwave surface resistance of MgB2. Applied Physics Letters, 2002, 80, 2347-2349.	3.3	29
144	The microwave surface impedance of MgB2thin films. Superconductor Science and Technology, 2003, 16, 1-6.	3.5	29

#	Article	IF	CITATIONS
145	All MOD buffer/YBCO approach to coated conductors. Physica C: Superconductivity and Its Applications, 2006, 445-448, 529-532.	1.2	29
146	Analytical modeling of residual stresses in multilayered superconductor systems. Journal of Materials Science, 2008, 43, 6223-6232.	3.7	29
147	Three-Dimensional Germanium Oxide Nanowire Networks. Crystal Growth and Design, 2009, 9, 35-39.	3.0	29
148	Studies on in situ magnetic alignment of bonded anisotropic Nd-Fe-B alloy powders. Journal of Magnetism and Magnetic Materials, 2017, 422, 168-173.	2.3	29
149	A perspective on conducting oxide buffers for Cu-based YBCO-coated conductors. Superconductor Science and Technology, 2006, 19, R23-R29.	3.5	28
150	Vapor-Phase Synthesis of Gallium Phosphide Nanowires. Crystal Growth and Design, 2009, 9, 525-527.	3.0	28
151	Fluorination of MXene by Elemental F <sub>2</sub> as Electrode Material for Lithiumâ€ <del>l</del> on Batteries. ChemSusChem, 2019, 12, 1316-1324.	6.8	28
152	Alternative Buffer Architectures for High Critical Current Density YBCO Superconducting Deposits on Rolling Assisted Biaxially-Textured Substrates. Japanese Journal of Applied Physics, 1999, 38, L178-L180.	1.5	27
153	Progress in solution-based YBCO coated conductor. Physica C: Superconductivity and Its Applications, 2001, 357-360, 987-990.	1.2	27
154	Enhanced flux pinning and critical currents in YBa2Cu3O7â^'δ films by nanoparticle surface decoration: Extension to coated conductor templates. Journal of Applied Physics, 2008, 104, 043906.	2.5	27
155	Humidity Effect on Nanoscale Electrochemistry in Solid Silver Ion Conductors and the Dual Nature of Its Locality. Nano Letters, 2015, 15, 1062-1069.	9.1	27
156	U.S. lithium resources from geothermal and extraction feasibility. Resources, Conservation and Recycling, 2021, 169, 105514.	10.8	27
157	Fabrication of high J/sub c/YBa/sub 2/Cu/sub 3/O//sub 7-γ/ tapes using the newly developed lanthanum manganate single buffer layers. IEEE Transactions on Applied Superconductivity, 2003, 13, 2481-2483.	1.7	26
158	Characterization of BaZrO3 Nanoparticles Prepared by Reverse Micelle Synthesis. Chemistry of Materials, 2005, 17, 4010-4017.	6.7	26
159	Sustainable Waste Tire Derived Carbon Material as a Potential Anode for Lithium-Ion Batteries. Sustainability, 2018, 10, 2840.	3.2	26
160	Surface barrier in Hg-based polycrystalline superconductors. Physical Review B, 1995, 51, 581-588.	3.2	25
161	Solution-processed lanthanum zirconium oxide as a barrier layer for high Ic-coated conductors. Journal of Materials Research, 2006, 21, 910-914.	2.6	25
162	Thermal stability of HfO2 nanotube arrays. Applied Surface Science, 2011, 257, 4075-4081.	6.1	25

#	Article	IF	CITATIONS
163	Review of additive manufacturing of permanent magnets for electrical machines: A prospective on wind turbine. Materials Today Physics, 2022, 24, 100675.	6.0	25
164	Thermoelectric power and resistivity of bulk HgBa2CuO4+y superconductors and the effects of annealing. Physica C: Superconductivity and Its Applications, 1994, 222, 47-51.	1.2	24
165	Thickness dependence of microstructure and critical current density of Yba2Cu3O7â^Ĵ on rolling-assisted biaxially textured substrates. Journal of Materials Research, 2003, 18, 1109-1122.	2.6	24
166	Solution processing of lanthanum zirconate films as single buffer layers for high I/sub c/ YBCO coated conductors. IEEE Transactions on Applied Superconductivity, 2003, 13, 2658-2660.	1.7	24
167	An approach for electrical self-stabilization of high-temperature superconducting wires for power applications. Applied Physics Letters, 2004, 85, 2887-2889.	3.3	24
168	Reel-to-reel x-ray diffraction and Raman microscopy analysis of differentially heat-treated Y–BaF2–Cu precursor films on metre-length RABiTS. Superconductor Science and Technology, 2004, 17, 739-749.	3.5	24
169	AC Losses in YBCO Coated Conductor With Inkjet Filaments. IEEE Transactions on Applied Superconductivity, 2007, 17, 3159-3162.	1.7	24
170	Magnetic order in CaMn2Sb2 studied via powder neutron diffraction. Journal of Magnetism and Magnetic Materials, 2009, 321, 3653-3657.	2.3	24
171	Modified Lanthanum Zirconium Oxide buffer layers for low-cost, high performance YBCO coated conductors. Physica C: Superconductivity and Its Applications, 2010, 470, 352-356.	1.2	24
172	Overcoming phase instability of RBaCo2O5+ $\hat{I}'$ (R=Y and Ho) by Sr substitution for application as cathodes in solid oxide fuel cells. Solid State Ionics, 2013, 253, 81-87.	2.7	24
173	Growth and characterization of oxide buffer layers for YBCO coated conductors. IEEE Transactions on Applied Superconductivity, 1999, 9, 1527-1530.	1.7	23
174	High critical current MOD ex situ YBCO films on RABiTSTM and MgO-IBAD templates. Physica C: Superconductivity and Its Applications, 2003, 390, 249-253.	1.2	23
175	Improved YBCO Coated Conductors Using Alternate Buffer Architectures. IEEE Transactions on Applied Superconductivity, 2005, 15, 2632-2634.	1.7	23
176	Germanium-catalyzed hierarchical Al2O3 and SiO2 nanowire bunch arrays. Nanoscale, 2009, 1, 347.	5.6	23
177	Phase stability and electrical conductivity of Ca-doped LaNb1â^'Ta O4â^' high temperature proton conductors. Journal of Power Sources, 2011, 196, 7395-7403.	7.8	23
178	Additive Manufacturing of Isotropic NdFeB PPS Bonded Permanent Magnets. Materials, 2020, 13, 3319.	2.9	23
179	Magneto-optical imaging of transport currents in YBa/sub 2/Cu/sub 3/O/sub 7-x/ on RABiTS/sup TM/. IEEE Transactions on Applied Superconductivity, 2001, 11, 3772-3775.	1.7	22
180	Growth of epitaxial Y2O3 buffer layers on biaxially textured Ni–W substrates for YBCO coated conductors by MOD approach. Physica C: Superconductivity and Its Applications, 2005, 422, 95-101.	1.2	22

#	Article	IF	CITATIONS
181	Strong flux-pinning in epitaxial NdBa2Cu3O7â^îÎfilms with columnar defects comprised of self-assembled nanodots of BaZrO3. Superconductor Science and Technology, 2006, 19, L42-L45.	3.5	22
182	MOD Buffer/YBCO Approach to Fabricate Low-Cost Second Generation HTS Wires. IEEE Transactions on Applied Superconductivity, 2007, 17, 3332-3335.	1.7	22
183	An integrated approach for structural characterization of complex solid state electrolytes: the case of lithium lanthanum titanate. Journal of Materials Chemistry A, 2014, 2, 2418.	10.3	22
184	High critical current density YBa <sub>2</sub> Cu <sub>3</sub> O <sub>7‑îî́</sub> coatings on LaMnO <sub>3</sub> -buffered biaxially textured Cu tapes for coated conductor applications. Journal of Materials Research, 2003, 18, 872-877.	2.6	21
185	Study of magnetization and pinning mechanisms in MgB2thin film superconductors: effect of heavy ion irradiation. Superconductor Science and Technology, 2003, 16, 951-955.	3.5	21
186	Improved textured La2Zr2O7 buffer on La3TaO7 seed for all-MOD Buffer/YBCO coated conductors. Physica C: Superconductivity and Its Applications, 2008, 468, 1587-1590.	1.2	21
187	Deposition studies and coordinated characterization of MOCVD YBCO films on IBAD-MgO templates. Superconductor Science and Technology, 2009, 22, 015008.	3.5	21
188	Size control of highly ordered HfO <sub>2</sub> nanotube arrays and a possible growth mechanism. Nanotechnology, 2009, 20, 455601.	2.6	21
189	Magnetic field orientation dependence of flux pinning in (Gd,Y)Ba2Cu3O7â^x coated conductor with tilted lattice and nanostructures. Physica C: Superconductivity and Its Applications, 2009, 469, 2044-2051.	1.2	21
190	(Y0.5In0.5)Ba(Co,Zn)4O7 cathodes with superior high-temperature phase stability for solid oxide fuel cells. Journal of Power Sources, 2012, 214, 7-14.	7.8	21
191	Polymer, Additives, and Processing Effects on N95 Filter Performance. ACS Applied Polymer Materials, 2021, 3, 1022-1031.	4.4	21
192	Laser-ablated epitaxial LaAlO3 buffer layers on biaxially textured Ni substrates for superconducting tapes. Physica C: Superconductivity and Its Applications, 1998, 304, 82-88.	1.2	20
193	Conductive buffer layers and overlayers for the thermal stability of coated conductors. IEEE Transactions on Applied Superconductivity, 2001, 11, 3309-3312.	1.7	20
194	Assessment of Chemical Solution Synthesis and Properties of Gd2Zr2O7 Thin Films as Buffer Layers for Second-Generation High-Temperature Superconductor Wires. Journal of Materials Research, 2005, 20, 2988-2996.	2.6	20
195	Studies of solution deposited cerium oxide thin films on textured Ni-alloy substrates for YBCO superconductor. Materials Research Bulletin, 2006, 41, 1063-1068.	5.2	20
196	Development of Solution Buffer Layers for RABiTS Based YBCO Coated Conductors. IEEE Transactions on Applied Superconductivity, 2011, 21, 3059-3061.	1.7	20
197	Neutron Spectroscopic and Thermochemical Characterization of Lithium–Aluminum-Layered Double Hydroxide Chloride: Implications for Lithium Recovery. Journal of Physical Chemistry C, 2019, 123, 20723-20729.	3.1	20
198	Synthesis and magnetic characterization of (Tl0.5Pb0.5)Sr2Ca2Cu3O9 and Tl2Ba2CaCu2O8 bulk superconductors. Physica C: Superconductivity and Its Applications, 1994, 219, 413-419.	1.2	19

#	Article	IF	CITATIONS
199	Pulsed electron deposition of fluorine-based precursors for YBa2Cu3O7â^'x-coated conductors. Superconductor Science and Technology, 2005, 18, 1168-1175.	3.5	19
200	Li <sub>6</sub> La <sub>3</sub> SnMO <sub>12</sub> (M = Sb, Nb, Ta), a Family of Lithium Garnets with High Li-Ion Conductivity. Journal of the Electrochemical Society, 2012, 159, A1148-A1151.	2.9	19
201	Neutron Diffraction and Electrochemical Studies of Na0.79CoO2and Na0.79Co0.7Mn0.3O2Cathodes for Sodium-Ion Batteries. Journal of the Electrochemical Society, 2014, 161, A961-A967.	2.9	19
202	Synthesis, characterization and electrochemical performance of Al-substituted Li2MnO3. Materials Science and Engineering B: Solid-State Materials for Advanced Technology, 2015, 201, 13-22.	3.5	19
203	Synthesis and characterization of substituted garnet and perovskite-based lithium-ion conducting solid electrolytes. Ionics, 2016, 22, 317-325.	2.4	19
204	Rationalization of solidification mechanism of Nd–Fe–B magnets during laser directed-energy deposition. Journal of Materials Science, 2018, 53, 8619-8626.	3.7	19
205	Life Cycle Assessment and Techno-Economic Assessment of Lithium Recovery from Geothermal Brine. ACS Sustainable Chemistry and Engineering, 2021, 9, 6551-6560.	6.7	19
206	Transport and structural characterization of epitaxial Nd1+xBa2â^'xCu3Oy thin films grown on LaAlO3 and Ni metal substrates by pulsed-laser deposition. Physica C: Superconductivity and Its Applications, 1999, 324, 177-186.	1.2	18
207	Epitaxy of HgBa2CaCu2O6 superconducting films on biaxially textured Ni substrates. Applied Physics Letters, 2000, 77, 4193-4195.	3.3	18
208	Growth and characterization of conductive SrRuO <sub>3</sub> and LaNiO <sub>3</sub> multilayers on textured Ni tapes for high-J <sub>c</sub> Yba <sub>2</sub> Cu <sub>3</sub> O <sub>7–delta;</sub> coated conductors. Journal of Materials Research, 2001, 16, 2661-2669.	2.6	18
209	Reelâ€toâ€Reel Continuous Chemical Solution Deposition of Epitaxial Gd <sub>2</sub> O <sub>3</sub> Buffer Layers on Biaxially Textured Metal Tapes for the Fabrication of YBa <sub>2</sub> Cu <sub>3</sub> O <sub>7â<sup>^</sup>Î</sub> Coated Conductors. Journal of the American Ceramic Society, 2003, 86, 257-265.	3.8	18
210	LaMnO/sub 3/: a single oxide buffer layer for high-J/sub c/ YBa/sub 2/Cu/sub 3/O//sub 7-γ/ coated conductors. IEEE Transactions on Applied Superconductivity, 2003, 13, 2661-2664.	1.7	18
211	Mesoporous TiO2 spheres with a nitridated conducting layer for lithium-ion batteries. Journal of Materials Science, 2013, 48, 5125-5131.	3.7	18
212	Alternating-current electrodeposition (metafuse) process for forming thallium-oxide superconductors. Physica C: Superconductivity and Its Applications, 1995, 251, 105-109.	1.2	17
213	Highâ€current superconducting Tl1Ba2Ca2Cu3Oy thick films on polycrystalline Ag by spin coating. Applied Physics Letters, 1995, 67, 294-296.	3.3	17
214	Title is missing!. Journal of Superconductivity and Novel Magnetism, 1998, 11, 159-161.	0.5	17
215	Atomic-Scale Picture of the Ion Conduction Mechanism in a Tetrahedral Network of Lanthanum Barium Gallate. Chemistry of Materials, 2013, 25, 2741-2748.	6.7	17
216	Novel Acid Catalysts from Wasteâ€Tireâ€Derived Carbon: Application in Waste–toâ€Biofuel Conversion. ChemistrySelect, 2017, 2, 4975-4982.	1.5	17

#	Article	IF	CITATIONS
217	Comparative photoemission studies ofTl2Ba2Canâ^'1CunO2n+4(n=1, 2, and 3). Physical Review B, 1993, 48, 15999-16005.	3.2	16
218	Direct growth of LaMnO <sub>3</sub> cap buffer layers on ion-beam-assisted deposition MgO for simplified template-based YBa <sub>2</sub> Cu <sub>3</sub> O <sub>7â^Î</sub> -coated conductors. Journal of Materials Research, 2008, 23, 3021-3028.	2.6	16
219	Structure and magnetic order in the series BixRE1â^'xFe0.5Mn0.5O3 (RE=La,Nd). Journal of Solid State Chemistry, 2011, 184, 830-842.	2.9	16
220	ZnO Doping and Defect Engineering—A Review. Springer Series in Materials Science, 2016, , 105-140.	0.6	16
221	Observing Framework Expansion of Ordered Mesoporous Hard Carbon Anodes with Ionic Liquid Electrolytes via in Situ Small-Angle Neutron Scattering. ACS Energy Letters, 2017, 2, 1698-1704.	17.4	16
222	Conversion of Waste Tire Rubber into High-Value-Added Carbon Supports for Electrocatalysis. Journal of the Electrochemical Society, 2018, 165, H881-H888.	2.9	16
223	Recycling of additively printed rare-earth bonded magnets. Waste Management, 2019, 90, 94-99.	7.4	16
224	Growth of Highly Oriented TlBa2Ca2Cu3O9-y Superconducting Films on Ag Substrates Using a Dip-Coated Barium Calcium Copper Oxide Sol-Gel Precursor. Journal of the American Ceramic Society, 1995, 78, 2551-2553.	3.8	15
225	Alternating transport-current flow in superconductive films: The role of a geometrical barrier to vortex motion. Physical Review B, 1999, 60, 6878-6883.	3.2	15
226	Electron beam co-evaporation of Y-BaF2-Cu precursor films for YBa2Cu3O7-ycoated conductors. Superconductor Science and Technology, 2001, 14, 218-223.	3.5	15
227	Investigation of TiN Seed Layers for RABiTS Architectures With a Single-Crystal-Like Out-of-Plane Texture. IEEE Transactions on Applied Superconductivity, 2005, 15, 2981-2984.	1.7	15
228	Processing Dependence of Texture, and Critical Properties of YBa2Cu3O7-delta Films on RABiTS Substrates by a Non-Fluorine MOD Method. Journal of the American Ceramic Society, 2006, 89, 914-920.	3.8	15
229	Enhanced Flux-Pinning in Dy-Doped, MOD YBCO Films on RABiTS. IEEE Transactions on Applied Superconductivity, 2007, 17, 3340-3342.	1.7	15
230	Superconducting properties of YBa <sub>2</sub> Cu <sub>3</sub> O <sub>7â^'î´</sub> films deposited on commercial tape substrates, decorated with Pd or Ta nano-islands. Superconductor Science and Technology, 2012, 25, 025018.	3.5	15
231	Facile Surface Coatings for Performance Improvement of NMC811 Battery Cathode Material. Journal of the Electrochemical Society, 2022, 169, 020565.	2.9	15
232	Single crystal studies of the pairing mechanism in Tl2Ba2CuO6 superconductors. Physica C: Superconductivity and Its Applications, 1993, 209, 199-202.	1.2	14
233	Preparation of textured YBCO films using all-iodide precursors. Physica C: Superconductivity and Its Applications, 1999, 319, 127-132.	1.2	14
234	Low temperature preparation of BaCeO3 and Ce0.75Zr0.25O2 thin films using sol-gel processing techniques. Materials Research Bulletin, 1999, 34, 817-825.	5.2	14

#	Article	IF	CITATIONS
235	Epitaxial superconducting Tl0.5Pb0.5Sr1.6Ba0.4Ca2Cu3O9films on LaAlO3by thermal spray and post-spray annealing. Superconductor Science and Technology, 1999, 12, L1-L4.	3.5	14
236	Synthesis and characterization of thallium-based 1212 films with high critical current density on LaAlO3substrates. Superconductor Science and Technology, 2000, 13, 173-177.	3.5	14
237	High Critical Current YBa2Cu3O7-delta Thick Films on Improved Rolling-Assisted Biaxially Textured Substrates (RABiTStm). Journal of the American Ceramic Society, 2005, 88, 2677-2680.	3.8	14
238	Growth of YBCO films on MgO-based rolling-assisted biaxially textured substrates templates. Superconductor Science and Technology, 2005, 18, 223-228.	3.5	14
239	Hole concentration and Tc in Tl2â^'yBa2Ca1â^'zYzCu2O8â^'x. Journal of Solid State Chemistry, 1992, 98, 343-349.	2.9	13
240	Optimization of buffer layers on rolled-Ni substrates for high current YBCO and Tl,Bi-1223 coated conductors using ex-situ precursor approaches. IEEE Transactions on Applied Superconductivity, 1999, 9, 2268-2271.	1.7	13
241	High-resolution transmission electron microscopy/analytical electron microscopy characterization of epitaxial oxide multilayers fabricated by laser ablation on biaxially textured Ni. Physica C: Superconductivity and Its Applications, 1999, 321, 29-38.	1.2	13
242	In-plane aligned superconducting Tl0.78Bi0.22Sr1.6Ba0.4Ca2Cu3O9 films on rolling assisted biaxially textured substrates. Physica C: Superconductivity and Its Applications, 1999, 313, 241-245.	1.2	13
243	Growth of rare-earth niobate-based pyrochlores on textured Ni–W substrates with ionic radii dependency. Journal of Materials Research, 2005, 20, 904-909.	2.6	13
244	Epitaxial Growth of Solution-Based Rare-Earth Niobate, RE3NbO7, Films on Biaxially Textured Ni–W Substrates. Journal of Materials Research, 2005, 20, 6-9.	2.6	13
245	Effect of Relative Humidity on the Crystallization of Solâ^'Gel Lanthanum Zirconium Oxide Films. Chemistry of Materials, 2006, 18, 5829-5831.	6.7	13
246	High temperature phase stabilities and electrochemical properties of InBaCo4â^'xZnxO7 cathodes for intermediate temperature solid oxide fuel cells. Electrochimica Acta, 2011, 56, 5740-5745.	5.2	13
247	Structure and Dynamics Investigations of Sr/Ca-Doped LaPO <sub>4</sub> Proton Conductors. Journal of Physical Chemistry C, 2017, 121, 11991-12002.	3.1	13
248	Carbon/tin oxide composite electrodes for improved lithium-ion batteries. Journal of Applied Electrochemistry, 2018, 48, 811-817.	2.9	13
249	Encapsulated Sb and Sb <sub>2</sub> O <sub>3</sub> particles in waste-tire derived carbon as stable composite anodes for sodium-ion batteries. Sustainable Energy and Fuels, 2020, 4, 3613-3622.	4.9	13
250	On the determination of hole concentration in thallium cuprate superconductors. Journal of Solid State Chemistry, 1992, 96, 464-467.	2.9	12
251	Hole concentration and critical temperature in the Tl2â^'xâ^'zBa2Ca2+xCu3O10â^'y system. Physica C: Superconductivity and Its Applications, 1992, 192, 161-165.	1.2	12
252	Structure and superconducting properties of (Tl0.8Bi0.2)(Sr1.6Ba0.4)Ca2Cu3O9â^î´. Physica C: Superconductivity and Its Applications, 1995, 253, 109-114.	1.2	12

#	Article	IF	CITATIONS
253	Preparation of Epitaxial YbBa2Cu3O7-δ on SrTiO3 Single Crystal Substrates Using a Solution Process. Japanese Journal of Applied Physics, 1999, 38, L727-L730.	1.5	12
254	Reel-to-reelex situconversion of high critical current density electron-beam co-evaporated BaF2precursor on RABiTS. Superconductor Science and Technology, 2004, 17, 386-394.	3.5	12
255	Solution Deposition Approach to High <tex>\$rm J_rm c\$</tex> Coated Conductor Fabrication. IEEE Transactions on Applied Superconductivity, 2005, 15, 2974-2976.	1.7	12
256	Formation of Highâ€Quality, Epitaxial La <sub>2</sub> Zr <sub>2</sub> O <sub>7</sub> Layers on Biaxially Textured Substrates by Slotâ€Die Coating of Chemical Solution Precursors. Journal of the American Ceramic Society, 2007, 90, 3529-3535.	3.8	12
257	Nano-engineered defect structures in Ce- and Ho-doped metal-organic chemical vapor deposited YBa2Cu3O6+δfilms: Correlation of structure and chemistry with flux pinning performance. Journal of Applied Physics, 2011, 109, 113923.	2.5	12
258	Monodispersed Li 4 Ti 5 O 12 with Controlled Morphology as High Power Lithium Ion Battery Anodes. ChemNanoMat, 2016, 2, 642-646.	2.8	12
259	Low-Field Alignment of Anisotropic Bonded Magnets for Additive Manufacturing of Permanent Magnet Motors. Jom, 2019, 71, 626-632.	1.9	12
260	Manufacturing Processes for Permanent Magnets: Part Il—Bonding and Emerging Methods. Jom, 2022, 74, 2492-2506.	1.9	12
261	Sol-Gel Synthesis of Rare Earth Aluminate Films as Buffer Layers for High Tc Superconducting Films. Materials Research Society Symposia Proceedings, 1997, 495, 263.	0.1	11
262	Reel-to-reel continuous deposition of epitaxial CeO/sub 2/ buffer layers on biaxially textured Ni tapes by electron beam evaporation. IEEE Transactions on Applied Superconductivity, 1999, 9, 1967-1970.	1.7	11
263	An all-sputtered buffer layer architecture for high-Jc YBa2Cu3O7â^î <sup>^</sup> coated conductors. Physica C: Superconductivity and Its Applications, 2000, 340, 33-40.	1.2	11
264	Microstructure of a high Jc, laser-ablated YBa2Cu3O7â^î́/sol–gel deposited NdGaO3 buffer layer/(001) SrTiO3 multi-layer structure. Physica C: Superconductivity and Its Applications, 2000, 331, 73-78.	1.2	11
265	Deposition of rare earth tantalate buffers on textured Ni-W substrates for YBCO coated conductor using chemical solution deposition approach. Journal of Materials Research, 2006, 21, 767-773.	2.6	11
266	Substrate Surface Decoration With \${m CeO}_{2}\$ Nanoparticles: An Effective Method for Improving Flux Pinning in \${m YBa}_{2}{m Cu}_{3}{m O}_{7-delta}\$ Films. IEEE Transactions on Applied Superconductivity, 2007, 17, 3720-3723.	1.7	11
267	Chemical Solution-Based Epitaxial Oxide Films on Biaxially Textured Ni-W Substrates with Improved Out-of-Plane Texture for YBCO-Coated Conductors. Journal of Electronic Materials, 2007, 36, 1270-1274.	2.2	11
268	Raman and x-ray absorption spectroscopy characterization of Zr-doped MOCVD YBa <sub>2</sub> Cu <sub>3</sub> O <sub>6+δ</sub> . Superconductor Science and Technology, 2010, 23, 014020.	3.5	11
269	Colloidal synthesis of BaF2 nanoparticles and their application as fillers in polymer nanocomposites. Applied Physics A: Materials Science and Processing, 2012, 106, 661-667.	2.3	11
270	Nanoparticle Shape Evolution and Proximity Effects During Tip-Induced Electrochemical Processes. ACS Nano, 2016, 10, 663-671.	14.6	11

#	Article	IF	CITATIONS
271	Low-cost combustion chemical vapor deposition of epitaxial buffer layers and superconductors. IEEE Transactions on Applied Superconductivity, 1999, 9, 2426-2429.	1.7	10
272	Synthesis and characterization of chromium-containing, thallium-based 1212 films. Physica C: Superconductivity and Its Applications, 2000, 333, 221-228.	1.2	10
273	Growth of high current density MgB2 films using ex-situ precursor approach. Physica C: Superconductivity and Its Applications, 2002, 378-381, 1252-1255.	1.2	10
274	Nonlinear microwave response of an MgB2thin film. Superconductor Science and Technology, 2004, 17, 681-684.	3.5	10
275	Strategic Buffer Layer Development for YBCO Coated Conductors. IEEE Transactions on Applied Superconductivity, 2009, 19, 3303-3306.	1.7	10
276	Second harmonic detection in the electrochemical strain microscopy of Ag-ion conducting glass. Applied Physics Letters, 2014, 105, 193106.	3.3	10
277	Quasi-Elastic Neutron Scattering Reveals Fast Proton Diffusion in Ca-Doped LaPO <sub>4</sub> . Journal of Physical Chemistry C, 2014, 118, 20112-20121.	3.1	10
278	Magnetic adsorbents for selective removal of selenite from contaminated water. Separation Science and Technology, 2019, 54, 2138-2146.	2.5	10
279	In-situ magnetic alignment model for additive manufacturing of anisotropic bonded magnets. Additive Manufacturing, 2021, 46, 102096.	3.0	10
280	Systematic thermopower behaviour in superconductors. Synthetic Metals, 1995, 71, 1583-1584.	3.9	9
281	Neutron diffraction studies on superconducting YNi2B2C at various temperatures. Physica B: Condensed Matter, 1996, 223-224, 105-108.	2.7	9
282	Progress towards a low-cost coated conductor technology. Physica C: Superconductivity and Its Applications, 2000, 341-348, 2319-2322.	1.2	9
283	Microstructural homogeneity and electromagnetic connectivity of YBa2Cu3O7â^´Î´ grown on rolling-assisted biaxially textured coated conductor substrates. Physica C: Superconductivity and Its Applications, 2000, 329, 114-120.	1.2	9
284	LED-induced fluorescence diagnostics for turbine and combustion engine thermometry. , 2001, 4448, 28.		9
285	R&D of RABiTS-based coated conductors: Conversion of ex situ YBCO superconductor using a novel pulsed electron-beam deposited precursor. Physica C: Superconductivity and Its Applications, 2005, 426-431, 878-886.	1.2	9
286	<tex>\$(rm La,rm Sr)rm TiO_3\$</tex> as a Conductive Buffer for High-Temperature Superconducting Coated Conductors. IEEE Transactions on Applied Superconductivity, 2005, 15, 2997-3000.	1.7	9
287	Development of Modified MOD-TFA Approach for YBCO Film Growth. IEEE Transactions on Applied Superconductivity, 2007, 17, 3557-3560.	1.7	9
288	Epitaxial growth of MgO/TiN multilayers on Cu. Vacuum, 2009, 83, 897-901.	3.5	9

#	Article	IF	CITATIONS
289	The influence of the local structure on proton transport in a solid oxide proton conductor La <sub>0.8</sub> Ba <sub>1.2</sub> GaO <sub>3.9</sub> . Journal of Materials Chemistry A, 2017, 5, 15507-15511.	10.3	9
290	Thermal and radiation response of 4H–SiC Schottky diodes with direct-write electrical contacts. Applied Physics Letters, 2020, 116, .	3.3	9
291	Enhanced flux pinning via chemical substitution in bulk superconducting Tl-2212. Superconductor Science and Technology, 1994, 7, 227-233.	3.5	8
292	Growth of TlBa <sub>2</sub> Ca <sub>2</sub> Cu <sub>3</sub> O <sub>9â^`<i>y</i></sub> superconducting films with local biaxial alignment extending up to 5 mm on Ag substrates using a spray-pyrolysis technique. Journal of Materials Research, 1997, 12, 619-623.	2.6	8
293	Thick-Film Processing for Tl-Oxide Wire and Tape. Journal of Superconductivity and Novel Magnetism, 1998, 11, 173-180.	0.5	8
294	Effective vortex pinning in MgB2thin films. Superconductor Science and Technology, 2002, 15, 1392-1397.	3.5	8
295	Defect chemistry of phospho-olivine nanoparticles synthesized by a microwave-assisted solvothermal process. Journal of Solid State Chemistry, 2013, 205, 197-204.	2.9	8
296	Proton dynamics in La0.8Ba1.2CaO3.9•nH2O studied by quasielastic incoherent neutron scattering. Solid State Ionics, 2013, 252, 12-18.	2.7	8
297	Neutron vibrational spectroscopic studies of novel tire-derived carbon materials. Physical Chemistry Chemical Physics, 2017, 19, 22256-22262.	2.8	8
298	Functionalizing magnet additive manufacturing with in-situ magnetic field source. Additive Manufacturing, 2020, 34, 101289.	3.0	8
299	Dynamics of Emim <sup>+</sup> in [Emim][TFSI]/LiTFSI Solutions as Bulk and under Confinement in a Quasi-liquid Solid Electrolyte. Journal of Physical Chemistry B, 2021, 125, 5443-5450.	2.6	8
300	Compression molding of anisotropic NdFeB bonded magnets in a polycarbonate matrix. Materialia, 2021, 19, 101167.	2.7	8
301	Band structures and Fermi surfaces of single- and double-Tl-O-layered high-temperature superconductors. Physical Review B, 1993, 47, 14489-14494.	3.2	7
302	Enhanced irreversibility field and current stabilization by Pb substitution in aligned Tl-1223 high-Tc superconductor. Physica C: Superconductivity and Its Applications, 1995, 253, 357-366.	1.2	7
303	Superconducting (TlBi)/sub 0.9/Sr/sub 1.6/Ba/sub 0.4/Ca/sub 2/Cu/sub 3/Ag/sub 0.2/O/sub x/ films from electrodeposited precursors. IEEE Transactions on Applied Superconductivity, 1999, 9, 1681-1683.	1.7	7
304	Continuous deposition of ex situ YBCO precursor films on rolling-assisted biaxially textured substrates by electron beam evaporation. Physica C: Superconductivity and Its Applications, 2001, 351, 175-181.	1.2	7
305	Study of the microwave electrodynamic response of MgB2 thin films. Physica C: Superconductivity and Its Applications, 2002, 372-376, 1287-1290.	1.2	7
306	Bulk solution techniques to fabricate high Jc YBCO coated conductors. Physica C: Superconductivity and Its Applications, 2002, 378-381, 1009-1012.	1.2	7

#	Article	IF	CITATIONS
307	A study on the nonlinear microwave electrodynamic response of e-beam evaporated MgB2superconducting thin films. Superconductor Science and Technology, 2003, 16, 260-263.	3.5	7
308	The growth of YBCO films with high critical current at reduced pressures using the BaF2ex situprocess. Superconductor Science and Technology, 2004, 17, 1209-1214.	3.5	7
309	Effects of Conversion Parameters on the Transport Properties of YBCO Films in the BaF2 Ex Situ Process. Journal of Materials Research, 2004, 19, 1281-1289.	2.6	7
310	An evaluation of phase separated, self-assembled LaMnO <sub>3</sub> -MgO nanocomposite films directly on IBAD-MgO as buffer layers for flux pinning enhancements in YBa <sub>2</sub> Cu <sub>3</sub> O <sub>7-1´</sub> coated conductors. Journal of Materials Research, 2010, 25, 437-443.	2.6	7
311	Evolution of structural and magnetic properties due to nanocrystallization of mechanically milled amorphous Pr-Co-B powders. Journal of Applied Physics, 2014, 116, .	2.5	7
312	Recent developments in filtration media and respirator technology in response to COVID-19. MRS Bulletin, 2021, 46, 822-831.	3.5	7
313	Microstructure of pulsed laser deposited YBa2Cu3O7â~î^ films on yttria-stabilized zirconia/CeO2 buffered biaxially textured Ni substrates. Physica C: Superconductivity and Its Applications, 2002, 377, 333-347.	1.2	6
314	Iridium: An Oxygen Diffusion Barrier and a Conductive Seed Layer for RABiTS-Based Coated Conted Conductors. IEEE Transactions on Applied Superconductivity, 2005, 15, 2977-2980.	1.7	6
315	Low ac loss geometries in YBCO coated conductors. Physica C: Superconductivity and Its Applications, 2007, 463-465, 755-760.	1.2	6
316	Phase-Separated, Epitaxial, Nanostructured LaMnO <sub>3</sub> +MgO Composite Cap Layer Films for Propagation of Pinning Defects in YBa <sub>2</sub> Cu <sub>3</sub> O <sub>7-Î</sub> Coated Conductors. Applied Physics Express, 0, 2, 063008.	2.4	6
317	Unraveling the structural properties and dynamics of sulfonated solid acid carbon catalysts with neutron vibrational spectroscopy. Catalysis Today, 2020, 358, 387-393.	4.4	6
318	Cryogenic heat capacity measurements and thermodynamic analysis of lithium aluminum layered double hydroxides (LDHs) with intercalated chloride. American Mineralogist, 2022, 107, 709-715.	1.9	6
319	<scp>3D</scp> printing of anisotropic <scp>Sm–Fe–N</scp> nylon bonded permanent magnets. Engineering Reports, 2021, 3, e12478.	1.7	6
320	Valence Charge Fluctuations in Tl2-x-zBa2Ca2+xCu3O10-y System. Journal of Solid State Chemistry, 1994, 109, 211-218.	2.9	5
321	Application of199Hg solid-state NMR to Hg based HTSC. Physica C: Superconductivity and Its Applications, 1994, 227, 225-229.	1.2	5
322	Field- and temperature-dependent surface resistance of superconducting polycrystalline multiple-phase Hg-Ba-Ca-Cu-O: Evidence for dirty-limit behavior. Physical Review B, 1995, 51, 3783-3790.	3.2	5
323	Properties of YBCO on \${m LaMnO}_{3}\$-Capped IBAD MgO-Templates Without Homo-Epitaxial MgO Layer. IEEE Transactions on Applied Superconductivity, 2009, 19, 3315-3318.	1.7	5
324	<i>In Situ</i> X-ray and Neutron Diffraction of the Rare-Earth Phosphate Proton Conductors Sr/Ca-Doped LaPO <sub>4</sub> at Elevated Temperatures. Chemistry of Materials, 2016, 28, 7232-7240.	6.7	5

#	Article	IF	CITATIONS
325	Conduction below 100°C in nominal Li6ZnNb4O14. Journal of Materials Science, 2016, 51, 854-860.	3.7	5
326	Fabrication and Characterization of Composite Membranes for the Concentration of Lithium Containing Solutions Using Forward Osmosis. Advanced Sustainable Systems, 2020, 4, 2000165.	5.3	5
327	Magnetic Sorbent for the Removal of Selenium(IV) from Simulated Industrial Wastewaters: Determination of Column Kinetic Parameters. Water (Switzerland), 2020, 12, 1234.	2.7	5
328	Preparation and magnetic properties of Cu6O8·InCl and LixCu6O8·InCl. Journal of Solid State Chemistry, 1992, 96, 243-246.	2.9	4
329	Buffer layers and thallination of Tl-based superconductors on flexible metal substrates. IEEE Transactions on Applied Superconductivity, 1999, 9, 1673-1676.	1.7	4
330	Growth of Lanthanum Manganate Buffer Layers for Coated Conductors via a Metal-Organic Decomposition Process. IEEE Transactions on Applied Superconductivity, 2005, 15, 3005-3008.	1.7	4
331	Slot Die Coating and Conversion of LZO on Rolling Assisted Biaxially Textured Ni-W Substrates With and Without a Very Thin Seed Layer in Low Vacuum. IEEE Transactions on Applied Superconductivity, 2007, 17, 3417-3419.	1.7	4
332	Alignment of magnetic particles in anisotropic Nd–Fe–B bonded magnets. Journal Physics D: Applied Physics, 2021, 54, 315004.	2.8	4
333	Valence band electronic structure of the Tl2â^'xâ^'zBa2Ca2+xCu3O10â^'y system. Physica C: Superconductivity and Its Applications, 1993, 214, 153-158.	1.2	3
334	Asymmetry between flux penetration and flux expulsion in Tl-2212 superconductors. Journal of Superconductivity and Novel Magnetism, 1993, 6, 185-189.	0.5	3
335	Evidence for phase stability and weak links in polycrystalline HgBa2CuO4 + δ. Applied Superconductivity, 1994, 2, 359-365.	0.5	3
336	199Hg and63,65Cu NMR studies of mercury based high-Tc superconductors. Applied Magnetic Resonance, 1995, 8, 57-65.	1.2	3
337	Fabrication, processing and properties of Tl-1223 conductors. IEEE Transactions on Applied Superconductivity, 1995, 5, 1405-1408.	1.7	3
338	Biaxially oriented metallic tape substrates for high-temperature superconductors. European Physical Journal D, 1996, 46, 1531-1532.	0.4	3
339	Buffer Layer R&D for YBCO Coated Conductor Composite Wires. AIP Conference Proceedings, 2004, , .	0.4	3
340	Optimization of a non-arsenic iron-based superconductor for wire fabrication. Superconductor Science and Technology, 2015, 28, 045018.	3.5	3
341	Effective antiviral coatings for deactivating SARS-CoV-2 virus on N95 respirator masks or filters. Materials Today Advances, 2022, 14, 100228.	5.2	3
342	Effect of site-selective substitution in bulk superconducting Tl2Ba2CaCu2O8. Journal of Electronic Materials, 1993, 22, 1205-1209.	2.2	2

M Parans Paranthaman

#	Article	IF	CITATIONS
343	Formation of anisotropic Tl-1212, Tl-2212, Tl-1223 and Tl-2223 particles using aerosol flow reacted powders. IEEE Transactions on Applied Superconductivity, 1995, 5, 1490-1493.	1.7	2
344	Interactions of Ba2YCu3O6+y with the Gd3NbO7 buffer layer in coated conductors. Journal of Solid State Chemistry, 2010, 183, 649-657.	2.9	2
345	Novel tri-modal defect structure in Nb-doped MOCVD Y Ba2Cu3O7: a paradigm for pinning landscape control. Superconductor Science and Technology, 2012, 25, 095013.	3.5	2
346	MADE3D: Enabling the next generation of high-torque density wind generators by additive design and 3D printing. Forschung Im Ingenieurwesen/Engineering Research, 2021, 85, 287-311.	1.6	2
347	Photoelectrochemical studies on Mo-cluster compounds, GaMo4S8 and ZnMo2Re2S8. Materials Research Bulletin, 1989, 24, 931-938.	5.2	1
348	Hole concentration and critical temperature in Tl2 –yBa2 –zLazCuO6 –x. Journal of Materials Chemistry, 1992, 2, 317-321.	6.7	1
349	Very Thin Films of High Dielectric Constant Materials. Materials Research Society Symposia Proceedings, 1996, 446, 309.	0.1	1
350	Solution Synthesis of Epitaxial Rare-Earth Oxide Thin Films on Roll-Textured Nickel. Materials Research Society Symposia Proceedings, 2000, 619, 203.	0.1	1
351	Single Buffer Layer Technology for YBCO Coated Conductors. Materials Research Society Symposia Proceedings, 2001, 689, 1.	0.1	1
352	Comparison of <tex>\$rm YBa_2rm Cu_3rm O_7-delta\$</tex> Precursors Made Using TFA-MOD and <tex>\$rm BaF_2\$</tex> Ex-Situ Processes and Their Post-Deposition Processing Under Low Pressure Conditions. IEEE Transactions on Applied Superconductivity, 2005, 15, 2659-2662.	1.7	1
353	Low-Cost Approaches for Flux-Pinning Enhancements in YBCO Films Using Solution Processing. IEEE Transactions on Applied Superconductivity, 2007, 17, 3668-3671.	1.7	1
354	Fabrication of High-\$J_{m c}\$\${m NdBa}_{2}{m Cu}_{3}{m O}_{7-delta}\$ and \${m BaZrO}_{3}\$-doped \${m NdBa}_{2}{m Cu}_{3}{m O}_{7-delta}\$ Films on RABiTS. IEEE Transactions on Applied Superconductivity, 2007, 17, 3672-3674.	1.7	1
355	Corrections to "Growth of Lanthanum Manganate Buffer Layers for Coated Conductors via a Metal–Organic Decomposition Process― IEEE Transactions on Applied Superconductivity, 2008, 18, 1801-1803.	1.7	1
356	Pinning Enhancements in YBCO Films via Nanoengineered \${m LaMnO}_{3}\$:\${m MgO}\$ Composite Cap Layer. IEEE Transactions on Applied Superconductivity, 2011, 21, 3171-3174.	1.7	1
357	Enhanced visible-light absorption of mesoporous TiO2 by co-doping with transition-metal/nitrogen ions. Materials Research Society Symposia Proceedings, 2013, 1547, 115-119.	0.1	1
358	Additively Manufactured NdFeB Polyphenylene Sulfide Halbach Magnets to Generate Variable Magnetic Fields for Neutron Reflectometry. 3D Printing and Additive Manufacturing, 0, , .	2.9	1
359	199Hg- solid state NMR and susceptibility studies of mercury - based HTSC. Physica C: Superconductivity and Its Applications, 1994, 235-240, 1671-1672.	1.2	0

360

#	Article	IF	CITATIONS
361	Equilibrium magnetic studies of Hg-based high-Tc superconductors. European Physical Journal D, 1996, 46, 1599-1600.	0.4	0
362	Progress towards a low-cost commercial coated conductor. Materials Research Society Symposia Proceedings, 2001, 689, 1.	0.1	0
363	Non-Fluorine Based Bulk Solution Techniques to Grow Superconducting YBa2Cu3O7â^î^ Films. , 2005, , 195-214.		0
364	Solution-derived textured oxide thin films—a review. Superconductor Science and Technology, 2009, 22, 049801-049801.	3.5	0
365	Fluorination of MXene by Elemental F <sub>2</sub> as Electrode Material for Lithiumâ€lon Batteries. ChemSusChem, 0, , .	6.8	0
366	Fluorination of MXene by Elemental F 2 as Electrode Material for Lithiumâ€lon Batteries. ChemSusChem, 2019, 12, 1271-1271.	6.8	0
367	(Invited) Carbon Nanostructures for Energy Storage Applications. ECS Meeting Abstracts, 2021, MA2021-01, 485-485.	0.0	0
368	Front Cover Image, Volume 3, Number 12, December 2021. Engineering Reports, 2021, 3, .	1.7	0
369	Thermal stability of anisotropic bonded magnets prepared by additive manufacturing. Journal of the American Ceramic Society, 0, , .	3.8	0